

Blue Phosphorescent Zwitterionic Iridium(III) Complexes Featuring Weakly Coordinating *nido*-Carborane-Based Ligands

Jonathan C. Axtell,^{†,‡} Kent O. Kirlikovali,^{†,‡} Peter I. Djurovich,[‡] Dahee Jung,[†] Vinh T. Nguyen,[†] Brian Munekiyo,[†] A. Timothy Royappa,^{§,||} Arnold L. Rheingold,[§] and Alexander M. Spokoyny^{*,†,⊥}

[†]Department of Chemistry and Biochemistry, University of California, Los Angeles, 607 Charles E. Young Drive East, Los Angeles, California 90095, United States

[‡]Department of Chemistry, University of Southern California, Los Angeles, California 90089, United States

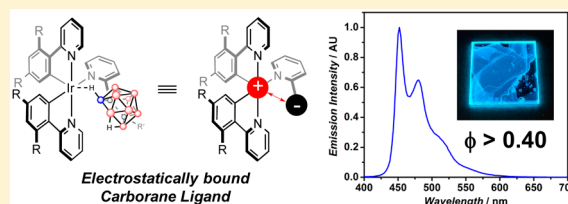
[§]Department of Chemistry, University of California, San Diego, 9500 Gilman Drive, La Jolla, California 92093, United States

^{||}Department of Chemistry, University of West Florida, 11000 University Parkway, Pensacola, Florida 32514, United States

[⊥]California NanoSystems Institute (CNSI), University of California, Los Angeles, 570 Westwood Plaza, Los Angeles, California 90095, United States

Supporting Information

ABSTRACT: We report the development of a new class of phosphorescent zwitterionic *bis*(heteroleptic) Ir(III) compounds containing pyridyl ligands with weakly coordinating *nido*-carboranyl substituents. Treatment of phenylpyridine-based Ir(III) precursors with C-substituted *ortho*-carboranylpyridines in 2-ethoxyethanol results in a facile carborane deboronation and the formation of robust and highly luminescent metal complexes. The resulting *nido*-carboranyl fragments associate with the cationic Ir(III) center through primarily electrostatic interactions. These compounds phosphoresce at blue wavelengths (450–470 nm) both in a poly(methyl methacrylate) (PMMA) matrix and in solution at 77 K. These complexes display structural stability at temperatures beyond 300 °C and quantum yields greater than 40%. Importantly, the observed quantum yields correspond to a dramatic 10-fold enhancement over the previously reported Ir(III) congeners featuring carboranyl-containing ligands in which the boron cluster is covalently attached to the metal. Ultimately, this work suggests that the use of a ligand framework containing a weakly coordinating anionic component can provide a new avenue for designing efficient Ir(III)-based phosphorescent emitters.



INTRODUCTION

The past two decades have seen a surge in the development of fluorescent¹ and phosphorescent² emitters with ever-increasing efficiency and color purity. In particular, the continued development of efficient Ir(III)-based phosphorescent compounds, currently targeted for their potential use in organic light-emitting diodes (OLEDs),³ represents a vital component of this research. Previous work has shown that ligand choice is crucial for optimizing luminescence efficiencies, emission wavelengths, and emitter stability in these devices (see Supporting Information (SI)).^{1,2} Still, despite the significant progress that has been made so far,⁴ efficient and long-lasting blue phosphorescent emitters have remained largely elusive.⁵

The prevailing design principle for Ir(III)-based phosphorescent systems leverages covalently bound strong- and weak-field (chelating) donor ligands to deliver the desired properties of the luminescent species (Figure 1A). This strategy would seem intuitive, given the well-recognized nonradiative decay pathways of excited-state Ir(III) species via ligand labilization/loss or excited-state distortions.⁶ Researchers have attempted to address this issue by using cyclometalated *N*-heterocyclic carbenes (NHCs) as L-type ligands to increase the energy barrier for nonradiative thermal deactivation.^{2f-h} In contrast to

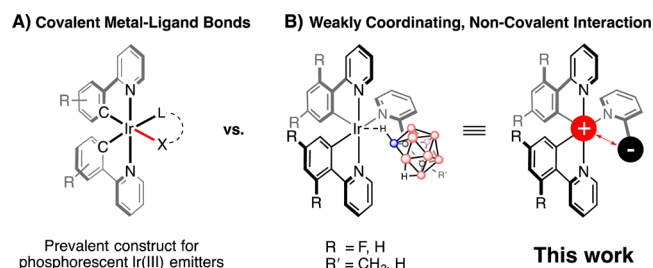


Figure 1. New design approach for luminescent metal complexes in which a weakly coordinating ligand is employed.

this convention, here we introduce a fundamentally new approach whereby strongly blue emitting and highly stable phosphorescent Ir(III) compounds are generated by employing weakly coordinating/noncovalently bound ligands derived from robust carborane clusters.

Carboranes,⁷ a class of icosahedral boron-based clusters recognized for their high stability⁸ and unique electronic

Received: September 29, 2016

Published: November 9, 2016

properties,^{9,10} have recently been utilized as ligand components of emissive Pt(II)- and Ir(III)-based molecules toward implementation as dopants in OLEDs¹¹ and as fluorophores in cell imaging.¹² The distinctive electronic influence of carboranes, which behave as electron-withdrawing groups if bound through carbon and electron-releasing groups if bound through boron, provide a unique opportunity for isosteric electronic variation.^{9,13} Since complete control over vertex functionalization of carboranes is still a largely unsolved problem, researchers in the field of OLED development have employed more easily accessible C-functionalized carborane scaffolds to perturb the electronic manifold of metal-based phosphors. However, despite the electronic extremes accessible through carborane as a ligand, very few¹⁴ phosphorescent metal-based molecules have been developed that contain carborane directly bound to a metal center or that contain deboronated (e.g., *nido*) analogues;¹⁵ rather, carboranyl substituents are most commonly installed on the periphery of the ligand scaffolds where direct interaction of the metal and the carborane is not possible (see SI for a brief summary of such emitters).¹⁶ As part of our ongoing studies of the organometallic chemistry of carboranes, we considered that deboronated carboranes, which are formally anionic, might be successfully employed as weakly coordinating/noncovalent ligands in building zwitterionic Ir(III)-based phosphorescent molecules.

RESULTS AND DISCUSSION

Synthesis. We began our studies in pursuit of generating *bis*(heteroleptic) Ir(III) phosphors with a *nido*-carboranylpyridine ligand. A common tactic employed in designing metal-based phosphorescent molecules involves the installation of strong field ligands such as carbanions or *N*-heterocyclic carbenes to stabilize metal-based orbitals; it is also known, however, that the filled *d*-orbitals may also be stabilized if electron density is removed from the metal center,¹⁷ either as a consequence of electron-withdrawing ligands or if the metal center bears a formal positive charge. In both cases, the HOMO–LUMO gaps are widened, opening the possibility for blue-shifted, radiative excited-state decay. We reasoned that the dominant steric profile of the *nido*-carboranyl scaffold amidst an otherwise rigid octahedral metal environment might minimize metal–cage interactions such that the metal holds a greater proportion of the formal positive charge. In addition, the diffuse nature of the negatively charged *nido*-carboranyl substituent would give poor directionality for interaction with the metal, thereby maintaining the desired ionic/noncovalent interaction by restricting electron sharing with the Ir(III) center.

To test this hypothesis, we synthesized ligand **1a**. The intermediate carboranylpyridine (Figure 2A, Compound **1b**) has been synthesized previously: one reported method requires Sonagashira coupling of 2-bromopyridine with dimethylethynyl carbinol, followed by condensation of 2-ethynylpyridine with decaborane, affording the desired product in ~28% yield (22% yield over two steps).¹⁸ More recently, Valliant and co-workers reported an alternative synthesis of **1b** from decaborane which requires the use of 10 mol % of a Ag(I)-based catalyst.¹⁹ Since C-metalated carboranyles (e.g., 1-Li-*o*-C₂B₁₀H₁₁) can easily be generated, we considered that such a species might be successfully employed in S_NAr-type reactivity with 2-fluoropyridine, a substrate documented to undergo substitution with a range of O-, N-, S-, and C-based nucleophiles.²⁰ Though few examples of electron-deficient arenes undergoing nucleophilic

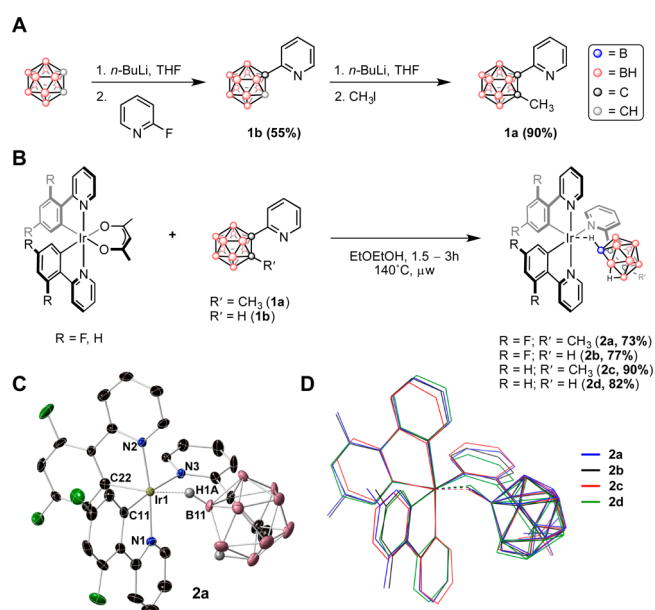


Figure 2. (A) Synthesis of carborane-based ligand precursors. (B) Ir(III) compounds containing a *nido*-carboranylpyridine ligand. (C) Solid-state structure of **2a** (carboranyl label corresponds to IUPAC numbering scheme). (D) Structure similarities of **2a–2d** are shown by superimposed stick models of the single crystal X-ray structures. Summary of the select bond distances and angles for structures **2a–2d** can be found in Figures S2 and S3 and Table S1.

substitution by metal carboranyl compounds exist²¹—none of which include heterocyclic arenes—we found that treatment of commercially available *o*-carborane with *n*-BuLi followed by addition of 2-fluoropyridine affords the desired ligand in a single step in 55% yield. Importantly, this protocol circumvents the use of the toxic decaborane precursor and metal-based catalysis. Subsequent deprotonation of **1b** followed by treatment with methyl iodide affords **1a** in good yield.

Treatment of Ir(^{F2}ppy)₂(acac)²² with **1a** under either microwave conditions or in an oil bath in 2-ethoxyethanol (EtOEtOH) for 3 h (Figure 2B) results in the formation of a golden yellow solution which emits blue under ultraviolet (UV) excitation (365 nm) at 77 K. Notably, this reaction is significantly faster and higher yielding than those generally observed for the synthesis of Ir(III) bis(heteroleptic) cyclo-metallates.^{2f} ¹¹B NMR spectroscopy revealed that the resulting product contained a deboronated carborane, which was identified from the diagnostic resonances in the –30 to –40 ppm range.

The solvent in this reaction was then removed *in vacuo*, and the resulting solid was subjected to additional spectroscopic characterization. The ¹H NMR spectrum of the sample dissolved in CDCl₃ showed diagnostic, upfield (~ –3.5 to –4.5 ppm) chemical shifts, characteristic of a hydride on the open face of a deboronated *o*-carborane. Precipitation of the Ir(III) species from hexanes afforded **2a** in 73% yield after purification. X-ray diffraction analysis of single crystals of the product (**2a**), grown from a concentrated EtOH solution at –15 °C, confirmed the presence of the *nido*-carboranyl group (Figure 2C). The deboronation of *o*-carborane is known to proceed through treatment with metal alkoxide or hydroxide bases in alcohol solvent;²³ we therefore suggest that the nature of the reaction solvent, in addition to the precoordination of **1a** to the Ir(III) center through pyridine, aids the observed

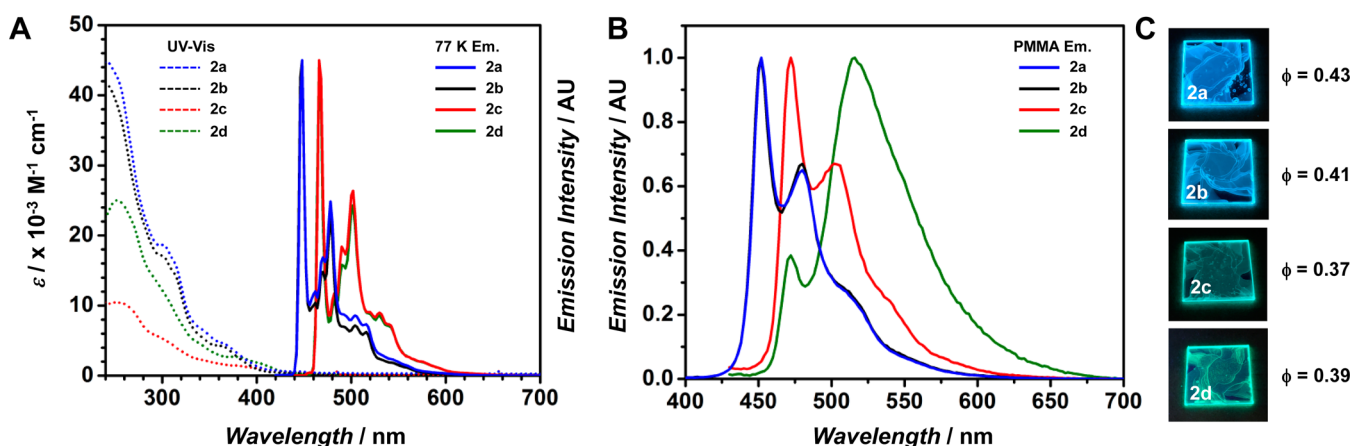


Figure 3. (A) UV-vis absorption (dotted line) and 77 K emission (solid line) spectra for **2a–2d**. UV-vis measurements were recorded in CH_2Cl_2 at 1×10^{-5} M, and 77 K emission spectra were obtained from solutions of 2-MeTHF. (B) Emission spectra of 2 wt % PMMA films of **2a–2d** ($\lambda_{\text{exc}} = 400$ nm). (C) Pictures of 2 wt % PMMA films of **2a–2d** when irradiated with UV light ($\lambda_{\text{exc}} = 365$ nm).

A	Abs. λ_{max}^a [$\epsilon \times 10^{-3}$ ($\text{M}^{-1}\text{cm}^{-1}$)]	Em. $\lambda_{\text{max}}^{b,c}$ (nm)	$\phi_{\text{PL}}^{b,d}$	$\tau^{b,e}$ (μs)	k_r^f ($\times 10^5 \text{ s}^{-1}$)	k_{nr}^f ($\times 10^5 \text{ s}^{-1}$)	k_r/k_{nr}
2a	253 [25], 338 [4.6], 279 [2.7]	452 (448)	0.43	3.35 (5.65)	1.3	1.7	0.76
2b	260 [10], 309 [4.7], 382 [1.4]	451 (447)	0.41	3.62 (6.38)	1.1	1.6	0.69
2c	244 [45], 302 [19], 367 [4.5]	472 (466)	0.37	3.02 (5.11)	1.2	2.1	0.57
2d	243 [41], 301 [17], 363 [4.3]	525 (466)	0.39	2.96 (5.19)	1.3	2.1	0.62
3a	255 [32], 306 [12], 377 [4.7]	463 (459)	0.070	0.62	1.1	15	0.07
3b	256 [39], 347 [6.4], 396.4.4]	489 (483)	0.035	0.71	0.49	14	0.04

B

R = F (**3a**)
R = H (**3b**)

○ = BH
● = C

Figure 4. (A) ^a UV-vis absorption spectra were measured in CH_2Cl_2 (1×10^{-5} M). ^b Emission maxima, quantum yields, and excited state lifetimes were measured in 2 wt % PMMA films. Spectra recorded in 2-MeTHF at 77 K are marked with parentheses. ^c Highest energy peaks are reported in this table. ^d Quantum yields were measured using an integrating sphere under N_2 . ^e Excited-state lifetime values in PMMA films are obtained from the weighted average of a biexponential decay. ^f Calculated for PMMA films according to the equations $k_r = \phi/\tau$ and $k_{\text{nr}} = (1 - \phi)/\tau$, where k_r is the radiative rate constant, k_{nr} is the nonradiative rate constant, ϕ is the quantum yield, and τ is the excited-state lifetime. (B) Structures of Ir(III) complexes featuring the covalently bound carboranyl ligand reported by Lee et al. (ref 14a).

deboronation.²⁴ Indeed, heating **1a** in EtOEtOH under the reaction conditions but in the absence of $\text{Ir}(\text{F}^2\text{ppy})_2(\text{acac})$ does not result in deboronation (or any other observable decomposition products). Additionally, heating $\text{Ir}(\text{F}^2\text{ppy})_2(\text{acac})$ and **1a** in a nonprotic solvent (1,2-dimethoxyethane or acetonitrile) under otherwise identical reaction conditions results in <10% conversion to **2a**.

In order to probe the effect of the *nido*-carboranyl ligand on the luminescent properties of Ir(III)-based compounds, we synthesized several derivatives featuring modified phenylpyridine (ppy) and carborane-based ligands. The deboronation of **1a** en route to formation of **2a** led us to question the necessity of protecting the remaining carboranyl C–H vertex of **1b**, particularly considering that C-functionalized *o*-carboranes containing electron-releasing substituents are generally more stable toward deboronation than the parent *o*-carborane.²⁵ **2b–2d** were synthesized in an analogous manner to **2a** (Figure 2B), and we find that no C–H activation is observed under the reaction conditions by using nonmethylated ligand **1b** as a precursor. X-ray crystallographic analysis of single crystals of **2b–2d** confirmed the presence of the *nido*-carboranyl ligand fragments as in **2a**. As expected, the structures of **2a–2d** are closely related, as seen from the superimposed wireframe plots shown in Figure 2D. Compound **2b**, which contains a proton at

the 2-position of the carborane cage, emits blue both in the solid state and in solution at 77 K under hand-held UV light. Compounds **2c** and **2d**, which contain unfunctionalized ppy ligands, emit blue-green in solution at 77 K under UV excitation (*vide infra*). **2d** also exhibits bright green emission in the solid state.

Photophysical Data. To our knowledge, **2a–2d** are the first examples of luminescent iridium(III) compounds that employ a cyclometalated ligand which associates with the metal through weakly coordinating/noncovalent interactions, despite a large number of cationic, luminescent iridium complexes having been reported. Many of these cationic Ir(III) species exist as formal salts,^{2g,26} while comparatively few zwitterionic species, which also contain formally cationic Ir(III) centers, have been documented.^{12,27} In contrast to **2a–2d**, the negatively charged component of these previously reported “inner-salt complexes”^{27a} is distal to the metal center and the coordination environment around the Ir(III) center falls in line with the more traditional construct containing covalent metal–ligand bonds (Figure 1A).

A suite of photophysical studies were carried out on **2a–2d** to evaluate the influence of the *nido*-carboranylpyridine ligand framework on the luminescent properties, excited state lifetime, and thermal stability of the title compounds. The absorption

and emission spectra of **2a–2d** are presented in Figure 3 with corresponding data presented in Figure 4A. All compounds exhibit strong absorption bands from 250–330 nm attributed to the spin-allowed $^1\pi-\pi^*$ transitions (^1LC) on the ppy ligands. The broad, lower intensity bands that extend from 340–420 nm arise from spin-allowed $^1\text{MLCT}$ and spin-forbidden $^3\text{MLCT}$ transitions that are consistent with previously reported Ir(III) complexes.²

All complexes are weakly emissive in fluid solutions of deaerated 2-MeTHF with quantum yields (ϕ) less than 0.01 at room temperature, but become strongly luminescent at 77 K and when doped in PMMA films (Figure 4A and SI). This behavior has been observed with other previously reported *mer*-Ir($\hat{\text{C}}\text{N}$)₃ ($\hat{\text{C}}\text{N}$ = cyclometalating ligand) complexes.^{2f} Interestingly, only **2b** and **2d**, which do not contain CH₃ groups bound to the 2-position of the *nido*-carboranyl fragment, exhibit observable emission as neat solids. This observation could also be ascribed to aggregation in the solid state due to a lesser degree of steric bulk on the carborane to prevent such interactions. A similar observation has been made by Lee and co-workers in Ir(III)-based emitters containing C-substituted carboranes.²⁸

At 298 K, the excited state lifetimes (τ) of **2a–2d** in fluid solution display multiexponential decays with nano- and microsecond components. The dynamic behavior suggests a possible equilibration between other triplet states before deactivation and is currently under further investigation. Upon cooling 2-MeTHF solutions of **2a–2d** to 77 K, τ becomes first-order and ranges from 5.11 μs (**2c**) to 6.38 μs (**2d**). Low temperature emission spectra for **2a–2d** all display well-defined vibronic features consistent with emission from a ligand-centered triplet state. Introduction of the CH₃ group to the *nido*-carboranyl-pyridyl ligand has a negligible effect on the luminescence, as the E_{0-0} energies and vibronic structure for **2a/2b** and **2c/2d** are nearly indistinguishable (Figure 3A). In PMMA films at room temperature the vibronic manifold in the emission spectra for **2a–c** red-shift and broaden relative to the corresponding spectra at 77 K (Figure 3B). In contrast, the low solubility for **2d** is evidenced in a spectrum that displays a broad, red-shifted band at 525 nm. This new feature indicates that **2d** aggregates prior to solvent evaporation despite filtering solutions before casting the PMMA film (see SI for further discussion). Indeed, Lee and co-workers have noted that substituted carboranyl components of Ir(III)-based emitters can help prevent solid-state quenching at higher concentrations.^{16f,h} The quantum yields for all four complexes drastically increase upon doping in PMMA films, ranging from 0.37 to 0.43 (Figure 4A).

Methylation of the *nido*-carboranyl fragment has little effect on photophysical properties when these complexes are doped in PMMA films since ϕ , τ , and the emission frequencies for **2a/2b** and **2c/2d** are roughly identical. Conveniently, the carboranyl moiety can be functionalized to address solubility issues, such as in the case of **2d** to **2c**, without significant effect on the emission properties. This is a significant advantage of the carborane-based framework in the context of the described system.

From the excited-state lifetimes and quantum yields of **2a–2d** doped in the PMMA matrices, the radiative (k_r) and nonradiative (k_{nr}) rate constants can be deduced (Figure 4A). The k_r values observed are between $1.1 \times 10^5 \text{ s}^{-1}$ and $1.3 \times 10^5 \text{ s}^{-1}$, with k_{nr} values ranging from $1.6 \times 10^5 \text{ s}^{-1}$ to $2.1 \times 10^5 \text{ s}^{-1}$. To elucidate the effect of the *nido*-carboranylpyridine ligand,

these values were compared to those of related complexes doped in PMMA films reported by Lee and co-workers, **3a** and **3b** (Figure 4B).^{14a} Though $\phi < 0.10$ for **3a** and **3b** in the PMMA films, the shorter τ values for these compounds yield k_r values roughly similar to those of **2a–2d**. In contrast, the k_{nr} values for **2a–2d** are more than an *order of magnitude lower* than those of **3a** and **3b**. The ratio of k_r/k_{nr} for **2d** is ~ 16 times greater than that for the related compound **3b** (0.64 and 0.04, respectively). Therefore, despite the weakly coordinating nature of the carboranyl fragment to the Ir(III), **2a–2d** exhibit significantly lower values for k_{nr} and hence up to a *10-fold increase* in quantum yields compared to values reported for related molecules with covalent Ir(III)–carborane interactions. This newly developed electrostatic framework thus potentially offers a counterintuitive yet useful concept in engineering efficient Ir(III) emitters for OLED devices.

Electrochemistry and Thermogravimetric Analysis.

Cyclic voltammetry (CV) plots of **2a–2c** are presented in Figure 5A with the associated data summarized in Table 1.

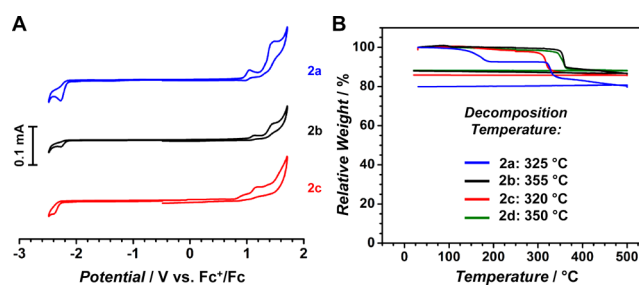


Figure 5. (A) Stacked cyclic voltammograms of **2a–2c** with scale bar of 0.1 mA. Referenced to Fc⁺/Fc in MeCN with a glassy carbon working electrode, scan rate = 0.1 V/s. Low solubility of **2d** prevented electrochemical characterization. (B) Thermogravimetric analysis (TGA) plots of **2a–2d** with corresponding temperatures of decomposition listed below. Mass loss at ~ 140 °C for **2a** corresponds to loss of residual EtOEtOH.

Table 1. Electrochemical Properties for 2a–2c and Related Compounds^{a,b}

compd	$V^{1/2}_{\text{Red}}$ (V)	$V^{1/2}_{\text{Ox},1}$ (V)	$V^{1/2}_{\text{Ox},2}$ (V)	ΔE (V) ^d
2a	−2.27	1.05	1.48	3.32
2b	−2.26	1.14	1.50	3.40
2c	−2.39	0.94	1.20	3.33
3a^e	−2.30	0.94 ^f	—	3.24
3b^e	−2.39	0.62 ^{c,f}	—	3.01

^aValues reported relative to the ferrocenium/ferrocene redox couple (Fc⁺/Fc) at 0.5 mM, scan rate = 0.1 V/s. ^bLow solubility of **2d** hindered electrochemical characterization. ^cReversible. ^d $\Delta E = V^{1/2}_{\text{Ox},1} - V^{1/2}_{\text{Red}}$. ^eFrom ref 14a. ^fValues correspond to first (and only) oxidation reported.

Compared to **3a** and **3b**, **2a–2c** have analogous reductive behavior as all complexes display a single, irreversible reduction wave from −2.26 V to −2.39 V versus the ferrocenium/ferrocene redox couple. Introduction of the methyl group on the *nido*-carboranyl ligand has negligible influence on the reduction potential, as $V^{1/2}_{\text{Red}}$ for **2a** and **2b** are 2.27 and 2.26 V, respectively. In contrast, the Ir(III) complexes bearing the *nido*-carboranyl ligands are up to 0.32 V more difficult to oxidize than their covalent analogues (**3a** and **3b**) and feature two irreversible oxidation waves. The first oxidation potential

($V^{1/2}_{\text{Ox},1}$) decreases from 1.14 V (**2b**) to 1.05 V (**2a**), likely due to the electron-releasing inductive effect of the methyl group. Furthermore, the second oxidation potential ($V^{1/2}_{\text{Ox},2}$) is roughly the same at 1.48 V for **2a** and 1.50 V for **2b**. On the basis of density functional theory (DFT) calculations (*vide infra*), reduction likely occurs on the ppy ligand,^{2f,29} whereas the two unique oxidations involve removal of an electron from both the *nido*-carboranyl fragment and the Ir(III) center.

A series of zwitterionic Ir(III)-based phosphors have been previously probed electrochemically^{27a} and were shown to display shifts to more positive potentials (1.09 V – 1.58 V vs Fc^+/Fc) compared to typical Ir(III)-based phosphors containing a formally neutral Ir(III) center (~ 0.9 V vs Fc^+/Fc). Cyclic voltammetry measurements of an independently synthesized deboronated analogue of **1b** (**4a**; see SI) were performed, which show the first oxidation wave centered at 0.57 V vs Fc^+/Fc . We therefore suggest that the first oxidation is centered on the *nido*-carboranyl fragment (whose oxidation is pushed to more positive potentials upon association to the metal center) and the second oxidation corresponds to a metal-centered Ir(III)/(IV) couple. Despite the apparent electrostatic interaction between the carboranyl ligand and the Ir(III) center, **2a–2d** have proven to be very thermally stable. Thermogravimetric analysis (TGA) shows the onset of mass loss occurring from 320–355 °C for these compounds (Figure S5B). Importantly, the introduction of methyl substitution on the carborane (**2a** and **2c**) does not significantly affect decomposition temperatures.

Structural and Computational Analysis. The electronic structures of **2a–2d** calculated using density functional theory (DFT) provide further insights into the observed photophysical phenomena. Ground-state geometries of **2a–2d** were optimized from the coordinates obtained from their crystallographically derived X-ray data, and subsequent single-point calculations were carried out with the B3LYP functional and TZP basis set (Figure 6A and 6B). The bond angles and distances of the optimized structures compare favorably with the experimentally determined metrics based on X-ray crystallography (Figure S4). The calculated energies corresponding to the first triplet excited state (T_1) to singlet ground state (S_0) are consistent with those measured in solution at 77 K (see SI for the summary of calculated values). As expected, the HOMO levels for **2a** and **2b**, which contain fluorinated ppy ligands, are located slightly lower in energy than those for **2c** and **2d**; similarly, the LUMO levels for **2a** and **2b** are slightly higher in energy than those for **2c** and **2d**. Finally, the experimentally observed emission data are consistent with the energy levels calculated for **2a–2d** (see SI, Table S3). Analysis of the solid state structure of **2a**, which will be treated in the following discussion as a representative example given the structural similarity of **2a–2d** (see Figure 2D and Figures S2 and S3), displays a *meridional* (*mer*) arrangement of the pyridine ligands. A long $\text{Ir}\cdots\text{B}(11)$ distance of 2.528(6) Å is found, which is longer than the sum of the covalent radii of the two atoms (2.07 Å) based on literature values,³⁰ suggesting no appreciable covalent metal–ligand bonding interaction. These distances are also systematically longer by ~ 0.3 Å than those in Ir(III)-based complexes in which B–H agostic interactions are normally invoked.^{31,32} In addition, the $\text{Ir–H}(1A)$ bond distance (1.935(9) Å) also well exceeds the sum of the covalent radii (1.54 Å) of Ir(III) and H atoms. The $\text{B}(11)\text{–H}(1A)$ bond distance of 1.007(2) Å is nearly identical to those of the other terminal B–H bonds on the boron cluster scaffold in **2a**,

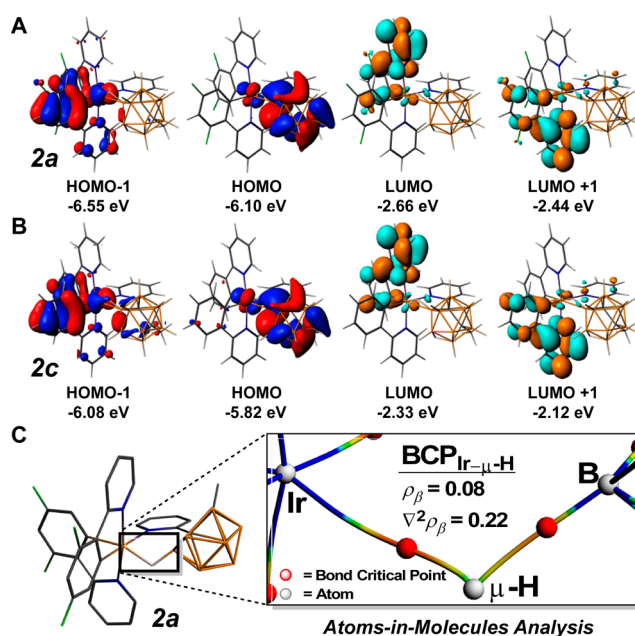


Figure 6. Frontier orbital diagrams of (A) **2a** and (B) **2c**. HOMO–1, HOMO, LUMO, and LUMO+1 diagrams were calculated from the geometry-optimized singlet state. (C) AIM analysis of **2a**. Electron density and Laplacian density values at the bond critical point suggest primarily electrostatic interactions between the *nido*-carboranyl fragment and the Ir(III) center.

suggesting that this bond (in addition to the analogous bonds in **2b–2d**) is not strongly activated by the Ir(III) center.

Infrared (IR) spectroscopy suggests only weak coordination of the bridging hydride to the metal center: solid-state IR spectra reveal broad resonances in the expected B–H region ~ 2500 cm^{-1} , which correspond to the cage B–H stretches, with some fine structure observed (Figure S7). An additional but very weak resonance is observed for **2a–2d**, ~ 2100 cm^{-1} , which is suggestive of a weak Ir– μ -H–B stretching band. Such M– μ -H–B interactions have been noted previously with carboranes.^{24b,32} In particular, Reed³³ and Teixidor³⁴ observed similar stretching frequencies in $[\text{CB}_{11}\text{H}_{12}]^-$ (~ 2380 cm^{-1}) and *nido*-carborane-based (2119–2077 cm^{-1}) systems, respectively, and have also ascribed these bands to weak interactions of carboranyl B–H bonds with cationic metal centers. Hawthorne observed slightly lower B–H stretching frequencies (~ 1965 cm^{-1}) for a *nido*-carborane anion associated with Ir(III) through two B– μ -H–Ir interactions.³⁵ Given the rigid steric profile of the ppy ligands around the octahedral iridium center and the bulk of the carboranyl ligand, we suggest that the bridging hydride interacts with the metal to complete its preferred octahedral geometry but that the primary mode of association results from ion pairing between the formally anionic *nido*-carborane and the formally cationic Ir(III) center (Figure 1B). ¹¹B NMR resonances for **2a–2c** (**2d** is too insoluble to observe defined ¹¹B signatures) contain several broad features at room temperature, where B–H coupling is not well-resolved. A variable temperature (VT) ¹¹B NMR study of **2a** revealed that these resonances further broaden upon cooling to -60 °C (see Figure S10) and sharpen upon heating to 60 °C, implicating fluxional behavior of the *nido*-carboranyl-metal interaction. At higher temperatures, it is revealed that one doublet in the ¹¹B NMR contains a slightly smaller coupling constant (~ 80 Hz) relative to the rest (~ 130 – 140 Hz); the ¹H

NMR also shows a partially resolved quartet (~ -3.5 ppm) with a $^1J_{\text{BH}}$ value of ~ 80 Hz. Given that the spectrum broadens upon cooling, the observation of this B–H coupling is a snapshot of a fluxional process that is fast on the NMR time scale and indicates that the M– μ -H–B is appreciable at some point during this dynamic process. Overall, these data support an electrostatic description interaction between the Ir(III) center and the *nido*-carboranyl ligand in the solid state and in solution as opposed to a covalent Ir–*nido*-carboranyl bond model.

Importantly, using DFT, we were able to further probe the interaction between Ir(III) and the *nido*-carboranyl fragment in **2a–2d** using the Quantum Theory of Atoms in Molecules (QTAIM) analysis, which has been used to evaluate different types of bonding (e.g., covalent, electrostatic) interactions between atoms.³⁶ The results suggest that minimal covalency exists between Ir(III) and either H(1A) or B(11) in **2a** (Figure 6C) or **2b–2d** (Table S4). First, no bond critical point (BCP) is observed between Ir and B(11) in any of the four title compounds. This is consistent with the long Ir–B(11) distances found crystallographically (which extend beyond the sum of the covalent radii of the two atoms) and further supports an electrostatic description of the interaction between the carboranyl ligand and the metal center as evidenced by the VT ¹¹B NMR study of **2a** (*vide supra*; see SI).

Second, while a BCP is found in **2a–2d** between Ir and H(1A), the value of the electron density (ρ_{β}) at this point is ~ 0.08 for all compounds. In general, ρ_{β} values of 0.2 or greater are indicative of covalent interactions, whereas values of less than 0.1 signify noncovalent interactions such as van der Waals, hydrogen bonding, or electrostatic interactions. The Laplacian of the electron density at the BCP ($\nabla^2\rho_{\beta}$) signifies the relative concentration or depletion of electron density along and perpendicular to the bond path at the BCP. Positive values generally indicate the depletion of electron density at the BCP, which is indicative of closed-shell bonding interactions, such as ionic and hydrogen bonding. Values of ~ 0.22 are obtained for all structures, strongly suggesting closed shell/electrostatic interactions between the carboranyl ligand fragment and Ir(III).

CONCLUSIONS

The concept of using electrostatically bound ligands for Ir(III)-based phosphors is introduced for the first time. The experimental and computational data suggest that the use of bulky, weakly coordinating, noncovalent ligand frameworks is a viable option for stable and emissive phosphorescent molecules based on Ir(III). Importantly, structural modification of the weakly coordinating ligand can be carried out without detrimentally affecting the photophysical properties of the resulting complex: the inclusion of a methyl group at the C-vertex of the *nido*-carboranyl ligand in **2a** and **2c** does not strongly influence the emission wavelength relative to the nonmethylated counterparts (**2b** and **2d**, respectively); importantly, however, methylation does improve the solubility of **2a** and **2c** relative to **2b** and **2d**. This orthogonality is a potentially useful handle for optimizing the physical/materials properties of this class of Ir(III)-based phosphors without significantly modulating the excited-state characteristics when employed as a component of an OLED construct, particularly given the nontriviality of engineering dopant–host layer compatibility.³⁷ Recent reports of straightforward methods to functionalize boron vertices of carboranes³⁸ with vertex precision also provide potentially powerful strategies for

modulating structural and photophysical properties of Ir(III) species with B-substituted carborane-based ligands. Ultimately, the utility of boron cluster-based weakly coordinating ligands in phosphorescent molecules demonstrated here sets the precedent for the exploration of this motif using other tunable boron cluster congeners that similarly present appreciable steric bulk and overall negative charge.³⁹ In particular, functionalized *closo*-boron clusters, such as the anionic carba-*closo*-dodecaboranes and charge-compensated *closo*-dodecaborates, are prime candidates for further study within this context, as these bulky, *closo*- clusters are generally more stable than *nido*- or *arachno*- derivatives and are themselves widely used as noncoordinating anions. A deeper understanding of the structure–function relationships of strategically designed, weakly coordinating carborane-based ligands on the materials and photophysical properties of metal-based luminescent molecules will potentially promote the discovery of new, efficient emitters for application in light-emitting devices.

ASSOCIATED CONTENT

Supporting Information

The Supporting Information is available free of charge on the ACS Publications website at DOI: 10.1021/jacs.6b10232.

Synthetic procedures for Ir(^{F2}ppy)₂(acac), Ir(ppy)₂(acac), **1a**, **1b**, **2a–2d**, and **4a**; spectroscopic characterization; crystallographic and computational data (PDF)

X-ray crystallographic data for **2a–2d** (CIF)

AUTHOR INFORMATION

Corresponding Author

*spokoiny@chem.ucla.edu

ORCID

Alexander M. Spokoiny: 0000-0002-5683-6240

Author Contributions

[#]J.C.A. and K.O.K. contributed equally.

Notes

The authors declare no competing financial interest.

ACKNOWLEDGMENTS

A.M.S. thanks the UCLA Department of Chemistry and Biochemistry for start-up funds, UCLA for a Faculty Career Development Award, and 3M for a Non-Tenured Faculty Award. The authors gratefully acknowledge Prof. Mark E. Thompson (USC) for use of instrumentation to collect photophysical data. The authors also thank Marco Messina (UCLA) for assistance with IR measurements and Dr. Greg Khitrov (UCLA) for assistance with mass spectral measurements.

REFERENCES

- (1) For selected examples of blue OLEDs incorporating fluorescent emitters, see: (a) Uoyama, H.; Goushi, K.; Shizu, K.; Nomura, H.; Adachi, C. *Nature* **2012**, *492*, 234. (b) Méhes, G.; Nomura, H.; Zhang, Q.; Nakagawa, T.; Adachi, C. *Angew. Chem., Int. Ed.* **2012**, *51*, 11311. (c) Lee, S. Y.; Yasuda, T.; Yang, Y. S.; Zhang, Q.; Adachi, C. *Angew. Chem., Int. Ed.* **2014**, *53*, 6402. (d) Kawasumi, K.; Wu, T.; Zhu, T.; Chae, H. S.; Van Voorhis, T.; Baldo, M. A.; Swager, T. M. *J. Am. Chem. Soc.* **2015**, *137*, 11908. (e) Zhang, Q.; Li, B.; Huang, S.; Nomura, H.; Tanaka, H.; Adachi, C. *Nat. Photonics* **2014**, *8*, 326. (f) Feuillastre, S.; Pauton, M.; Gao, L.; Desmarchelier, A.; Riives, A. J.; Prim, D.; Tondelier, D.; Geffroy, B.; Muller, G.; Clavier, G.; Pieters, G. *J. Am.*

Chem. Soc. **2016**, *138*, 3990. (g) Li, K.; Guan, X.; Ma, C.-W.; Chen, Y.; Che, C.-M. *Chem. Commun.* **2011**, *47*, 9075.

(2) For selected examples of phosphorescent emitters for OLED applications, see: (a) Yersin, H., Ed. *Highly Efficient OLEDs with Phosphorescent Materials*; Wiley-VCH: Weinheim, 2008. (b) Chou, P.-T.; Chi, Y. *Chem. - Eur. J.* **2007**, *13*, 380. (c) Chi, Y.; Chou, P.-T. *Chem. Soc. Rev.* **2010**, *39*, 638. (d) Lamansky, S.; Djurovich, P.; Murphy, D.; Abdel-Razzaq, F.; Lee, H.-E.; Adachi, C.; Burrows, P. E.; Forrest, S. R.; Thompson, M. E. *J. Am. Chem. Soc.* **2001**, *123*, 4304. (e) Lamansky, S.; Djurovich, P.; Murphy, D.; Abdel-Razzaq, F.; Kwong, R.; Tsyba, I.; Bortz, M.; Mui, B.; Bau, R.; Thompson, M. E. *Inorg. Chem.* **2001**, *40*, 1704. (f) Tamayo, A. B.; Alleyne, B. D.; Djurovich, P. I.; Lamansky, S.; Tsyba, I.; Ho, N. N.; Bau, R.; Thompson, M. E. *J. Am. Chem. Soc.* **2003**, *125*, 7377. (g) Sajoto, T.; Djurovich, P. I.; Tamayo, A.; Yousufuddin, M.; Bau, R.; Thompson, M. E. *Inorg. Chem.* **2005**, *44*, 7992. (h) Chang, C.-F.; Cheng, Y.-M.; Chi, Y.; Chiu, Y.-C.; Lin, C.-C.; Lee, G.-H.; Chou, P.-T.; Chen, C.-C.; Chang, C.-H.; Wu, C.-C. *Angew. Chem., Int. Ed.* **2008**, *47*, 4542. (i) Tsuboyama, A.; Iwawaki, H.; Furugori, M.; Mukaide, T.; Kamatani, J.; Igawa, S.; Moriyama, T.; Miura, S.; Takiguchi, T.; Okada, S.; Hoshino, M.; Ueno, K. *J. Am. Chem. Soc.* **2003**, *125*, 12971. (j) Maity, A.; Le, L. Q.; Zhu, Z.; Bao, J.; Teets, T. S. *Inorg. Chem.* **2016**, *55*, 2299. (k) Fleetham, T.; Wang, Z.; Li, J. *Org. Electron.* **2012**, *13*, 1430. (l) Turner, E.; Bakken, N.; Li, J. *Inorg. Chem.* **2013**, *52*, 7344. (m) Saris, P. J. G.; Thompson, M. E. *Org. Lett.* **2016**, *18*, 3960. (n) Kui, S. C. F.; Chow, P. K.; Cheng, G.; Kwok, C.-C.; Kwong, C. L.; Low, K.-H.; Che, C.-M. *Chem. Commun.* **2013**, *49*, 1497. (o) Hudson, Z. M.; Sun, C.; Helander, M. G.; Amarné, H.; Lu, Z.-H.; Wang, S. *Adv. Funct. Mater.* **2010**, *20*, 3426. (p) Ko, S.-B.; Park, H.-J.; Gong, S.; Wang, X.; Lu, Z.-H.; Wang, S. *Dalton Trans.* **2015**, *44*, 8433.

(3) Tremblay, J.-F. The rise of OLED displays. *Chemical & Engineering News*, July 11, 2016; pp 30–34 (URL: <http://cen.acs.org/articles/94/i28/rise-OLED-displays.html>).

(4) (a) Zhang, Y.; Lee, J.; Forrest, S. R. *Nat. Commun.* **2014**, *5*, 5008. (b) Fleetham, T.; Li, G.; Wen, L.; Li, J. *Adv. Mater.* **2014**, *26*, 7116. (c) Lee, J.; Chen, H.-F.; Batagoda, T.; Coburn, C.; Djurovich, P. I.; Thompson, M. E.; Forrest, S. R. *Nat. Mater.* **2015**, *15*, 92. (d) Fleetham, T. B.; Huang, L.; Klimes, K.; Brooks, J.; Li, J. *Chem. Mater.* **2016**, *28*, 3276.

(5) (a) Giebink, N. C.; D'Andrade, B. W.; Weaver, M. S.; Mackenzie, P. B.; Brown, J. J.; Thompson, M. E.; Forrest, S. R. *J. Appl. Phys.* **2008**, *103*, 044509. (b) Seifert, R.; de Moraes, I. R.; Scholz, S.; Gather, M. C.; Lüssem, B.; Leo, K. *Org. Electron.* **2013**, *14*, 115. (c) Holmes, R. J.; Forrest, S. R.; Tung, Y.-J.; Kwong, R. C.; Brown, J. J.; Garon, S.; Thompson, M. *Appl. Phys. Lett.* **2003**, *82*, 2422.

(6) (a) Sajoto, T.; Djurovich, P. I.; Tamayo, A. B.; Oxgaard, J.; Goddard, W. A., III; Thompson, M. E. *J. Am. Chem. Soc.* **2009**, *131*, 9813. (b) Zhou, X.; Burn, P. L.; Powell, B. J. *Inorg. Chem.* **2016**, *55*, 5266. (c) Yang, L.; Okuda, F.; Kobayashi, K.; Nozaki, K.; Tanabe, Y.; Ishii, Y.; Haga, M. *Inorg. Chem.* **2008**, *47*, 7154.

(7) (a) Heying, T. L.; Ager, J. W., Jr.; Clark, S. L.; Mangold, D. J.; Goldstein, H. L.; Hillman, M.; Polak, R. J.; Szymanski, J. W. *Inorg. Chem.* **1963**, *2*, 1089. (b) Fein, M. M.; Grafstein, D.; Paustian, J. E.; Bobinski, J.; Lichstein, B. M.; Mayes, N.; Schwartz, N. N.; Cohen, M. S. *Inorg. Chem.* **1963**, *2*, 1115. (c) Fein, M. M.; Bobinski, J.; Mayes, N.; Schwartz, N.; Cohen, M. S. *Inorg. Chem.* **1963**, *2*, 1111. (d) Zakharkin, L. I.; Stanki, V. I.; Brattsev, V. A.; Chapovskii, Y. A.; Klimova, A. I.; Okhlobystin, O. Y.; Ponomarenko, A. A. *Dokl. Akad. Nauk. SSSR* **1964**, *155*, 1119. (e) Hawthorne, M. F.; Andrews, T. D.; Garrett, P. M.; Olsen, F. P.; Reintjes, M.; Tebbe, F. N.; Warren, L. F.; Wegner, P. A.; Young, D. C. *Inorg. Synth* **1967**, *10*, 91. (f) Grimes, R. N. *Carboranes*, 3rd ed; Academic Press: 2016.

(8) (a) Lipscomb, W. N. *Boron Hydrides*; Benjamin: New York, 1963. (b) Schleyer, P. v. R.; Najafian, K. *Inorg. Chem.* **1998**, *37*, 3454. (c) Chen, Z.; King, R. B. *Chem. Rev.* **2005**, *105*, 3613. (d) King, R. B. *Chem. Rev.* **2001**, *101*, 1119.

(9) Spokoyny, A. M.; Machan, C. W.; Clingerman, D. J.; Rosen, M. S.; Wiester, M. J.; Kennedy, R. D.; Stern, C. L.; Sarjeant, A. A.; Mirkin, C. A. *Nat. Chem.* **2011**, *3*, 590.

(10) (a) Grimes, R. N. *Dalton Trans.* **2015**, *44*, 5939. (b) Tsang, M. Y.; Viñas, C.; Teixidor, F.; Planas, J. G.; Conde, N.; SanMartin, R.; Herrero, M. T.; Domínguez, E.; Lledós, A.; Vidossich, P.; Choquesillo-Lazarte, D. *Inorg. Chem.* **2014**, *53*, 9284. (c) Gabel, D. *Pure Appl. Chem.* **2015**, *87*, 173. (d) Teixidor, F.; Sillanpää, R.; Pepiol, A. *Chem. - Eur. J.* **2015**, *21*, 12778. (e) Eleazer, B. J.; Smith, M. D.; Peryshkov, D. V. *Organometallics* **2016**, *35*, 106. (f) Schwartz, J. J.; Mendoza, M. A.; Wattanatorn, N.; Zhao, Y.; Nguyen, V. T.; Spokoyny, A. M.; Mirkin, C. A.; Baše, T.; Weiss, P. S. *J. Am. Chem. Soc.* **2016**, *138*, 5957. (g) Kennedy, R. D.; Peng, Y.; Clingerman, D. J.; Mondloch, J.; Krungleviciute, V.; Wilmer, C. E.; Sarjeant, A. A.; Snurr, J.; Hupp, T.; Yildirim, T.; Farha, O. K.; Mirkin, C. A. *Chem. Mater.* **2013**, *25*, 3539.

(11) (a) Mukherjee, S.; Thilagar, P. *Chem. Commun.* **2016**, *52*, 1070. (b) Li, X.; Yan, H.; Zhao, Q. *Chem. - Eur. J.* **2016**, *22*, 1888. (c) Kirlikovali, K. O.; Axtell, J. C.; Gonzalez, A.; Phung, A. C.; Khan, S. I.; Spokoyny, A. M. *Chem. Sci.* **2016**, *7*, 5132.

(12) Jiang, W.; Gao, Y.; Sun, Y.; Ding, F.; Xu, Y.; Bian, Z.; Li, F.; Bian, J.; Huang, C. *Inorg. Chem.* **2010**, *49*, 3252.

(13) (a) Weller, A. *Nat. Chem.* **2011**, *3*, 577. (b) Spokoyny, A. M.; Lewis, C. D.; Teverovskiy, G.; Buchwald, S. L. *Organometallics* **2012**, *31*, 8478.

(14) (a) Bae, H. J.; Kim, H.; Lee, K. M.; Kim, T.; Eo, M.; Lee, Y. S.; Do, Y.; Lee, M. H. *Dalton Trans.* **2013**, *42*, 8549. (b) Kim, T.; Lee, J.; Lee, S. U.; Lee, M. H. *Organometallics* **2015**, *34*, 3455. (c) Prokhorov, A. M.; Slepukhin, P. A.; Rusinov, V. L.; Kalinin, V. N.; Kozhevnikov, D. N. *Chem. Commun.* **2011**, *47*, 7713. (d) Prokhorov, A. M.; Hofbeck, T.; Czerwieńiec, R.; Suleymanova, A. F.; Kozhevnikov, D. N.; Yersin, H. *J. Am. Chem. Soc.* **2014**, *136*, 9637.

(15) (a) Shi, C.; Tu, D.; Yu, Q.; Liang, H.; Liu, Y.; Li, Z.; Yan, H.; Zhao, Q.; Huang, W. *Chem. - Eur. J.* **2014**, *20*, 16550. (b) Visbal, R.; Ospino, I.; López-de-Luzuriaga, J. M.; Laguna, A.; Gimeno, M. C. *J. Am. Chem. Soc.* **2013**, *135*, 4712. (c) Visbal, R.; López-de-Luzuriaga, J. M.; Laguna, A.; Gimeno, M. C. *Dalton Trans.* **2014**, *43*, 328. (d) Czerwieńiec, R.; Hofbeck, T.; Crespo, O.; Laguna, A.; Gimeno, M. C.; Yersin, H. *Inorg. Chem.* **2010**, *49*, 3764. (e) Crespo, O.; Gimeno, M. C.; Jones, P. G.; Laguna, A.; López-de-Luzuriaga, J. M.; Monge, M.; Pérez, J. L.; Ramón, M. A. *Inorg. Chem.* **2003**, *42*, 2061. (f) Crespo, O.; Gimeno, M. C.; Laguna, A.; Lehtonen, O.; Ospino, I.; Pyykkö, P.; Villacampa, M. D. *Chem. - Eur. J.* **2014**, *20*, 3120.

(16) (a) Shi, C.; Sun, H.; Jiang, Q.; Zhao, Q.; Wang, J.; Huang, W.; Yan, H. *Chem. Commun.* **2013**, *49*, 4746. (b) Kim, T.; Kim, H.; Lee, K. M.; Lee, Y. S.; Lee, M. H. *Inorg. Chem.* **2013**, *52*, 160. (c) Shi, C.; Sun, H.; Tang, X.; Lv, W.; Yan, H.; Zhao, Q.; Wang, J.; Huang, W. *Angew. Chem., Int. Ed.* **2013**, *52*, 13434. (d) Lee, Y. H.; Park, J.; Lee, J.; Lee, S. U.; Lee, M. H. *J. Am. Chem. Soc.* **2015**, *137*, 8018. (e) Zhu, L.; Tang, X.; Yu, Q.; Lv, W.; Yan, H.; Zhao, Q.; Huang, W. *Chem. - Eur. J.* **2015**, *21*, 4721. (f) Lee, Y. H.; Park, J.; Jo, S.-J.; Kim, M.; Lee, J.; Lee, S. U.; Lee, M. H. *Chem. - Eur. J.* **2015**, *21*, 2052. (g) Park, J.; Lee, Y. H.; Ryu, J. Y.; Lee, J.; Lee, M. H. *Dalton Trans.* **2016**, *45*, 5667. (h) Kim, Y.; Park, S.; Lee, Y. H.; Jung, J.; Yoo, S.; Lee, M. H. *Inorg. Chem.* **2016**, *55*, 909.

(17) Li, J.; Djurovich, P. I.; Alleyne, B. D.; Tsyba, I.; Ho, N. N.; Bau, R.; Thompson, M. E. *Polyhedron* **2004**, *23*, 419.

(18) (a) Ames, D. E.; Bull, D.; Takundwa, C. *Synthesis* **1981**, 1981, 364. (b) Coult, F.; Fox, M. A.; Gill, W. R.; Herbertson, P. L.; MacBride, J. A. H.; Wade, K. J. *Organomet. Chem.* **1993**, *462*, 19.

(19) El-Zaria, M. E.; Keskar, K.; Genady, A. F.; Ioppolo, J. A.; McNulty, J.; Valliant, J. F. *Angew. Chem., Int. Ed.* **2014**, *53*, 5156.

(20) (a) Fort, Y.; Forgione, P. 2-Fluoropyridine. *E-Eros Encyclopedia of Reagents for Organic Synthesis*; 2007. (b) Cheng, Y.-J. *Tetrahedron* **2002**, *58*, 4931.

(21) (a) Zakharkin, L. I.; Lebedev, V. N. *Bull. Acad. Sci. USSR, Div. Chem. Sci.* **1970**, *19*, 914. (b) Zakharkin, L. I.; Lebedev, V. N. *Bull. Acad. Sci. USSR, Div. Chem. Sci.* **1972**, *21*, 2273. (c) Henly, T. J.; Knobler, C. B.; Hawthorne, M. F. *Organometallics* **1992**, *11*, 2313. (d) Ohta, K.; Ogawa, T.; Endo, Y. *Bioorg. Med. Chem. Lett.* **2012**, *22*, 4728. (e) Tricas, H.; Colon, M.; Ellis, D.; Macgregor, S. A.; McKay, D.; Rosair, G. M.; Welch, A. J.; Glukhov, I. V.; Rossi, F.; Laschi, F.;

- Zanello, P. *Dalton Trans.* **2011**, 40, 4200. (f) Ohta, K.; Goto, R.; Endo, Y. *Tetrahedron Lett.* **2005**, 46, 483.
- (22) Lamansky, S.; Djurovich, P. I.; Murphy, D.; Abdel-Razzaq, F.; Kwong, R.; Tsyba, I.; Bortz, M.; Mui, B.; Bau, R.; Thompson, M. E. *Inorg. Chem.* **2001**, 40, 1704 (see SI for NMR characterization).
- (23) (a) Wiesboeck, R. A.; Hawthorne, M. F. *J. Am. Chem. Soc.* **1964**, 86, 1642. (b) Hawthorne, M. F.; Young, D. C.; Garrett, P. M.; Owen, D. A.; Schwerin, S. G.; Tebbe, F. N.; Wegner, P. A. *J. Am. Chem. Soc.* **1968**, 90, 862. (c) Plešek, J.; Heřmánek, S.; Štibr, B.; Waksman, L.; Sneddon, L. G. *Inorg. Synth* **1984**, 22, 231.
- (24) (a) Sit, M.-M.; Chan, H.-S.; Xie, Z. *Organometallics* **2011**, 30, 3449. (b) Teixidor, F.; Núñez, R.; Flores, M. A.; Demonceau, A.; Viñas, C. *J. Organomet. Chem.* **2000**, 614–615, 48.
- (25) (a) Zakharkin, L. I.; Kirillova, V. S. *Bull. Acad. Sci. USSR, Div. Chem. Sci.* **1975**, 24, 2484. (b) Schaeck, J. J.; Kahl, S. B. *Inorg. Chem.* **1999**, 38, 204.
- (26) Ladouceur, S.; Zysman-Colman, E. *Eur. J. Inorg. Chem.* **2013**, 2013, 2985.
- (27) (a) Darmawan, N.; Yang, C.-H.; Mauro, M.; Frohlich, R.; De Cola, L.; Chang, C.-H.; Wu, Z.-J.; Tai, C.-W. *J. Mater. Chem. C* **2014**, 2, 2569. (b) Byun, Y.; Lyu, Y.-Y.; Das, R. R.; Kwon, O.; Lee, T.-W.; Park, Y. *J. Appl. Phys. Lett.* **2007**, 91, 211106. (c) Jiang, W.; Gao, Y.; Sun, Y.; Ding, F.; Xu, Y.; Bian, Z.; Li, F.; Bian, J.; Huang, C. *Inorg. Chem.* **2010**, 49, 3252. (d) Li, J.; Djurovich, P. I.; Alleyne, B. D.; Tsyba, I.; Ho, N. N.; Bau, R.; Thompson, M. E. *Polyhedron* **2004**, 23, 419.
- (28) Bae, H. J.; Chung, J.; Kim, H.; Park, J.; Lee, K. M.; Koh, T.-W.; Lee, Y. S.; Yoo, S.; Do, Y.; Lee, M. H. *Inorg. Chem.* **2014**, 53, 128.
- (29) Dedeian, K.; Shi, J.; Shepherd, N.; Forsythe, E.; Morton, D. C. *Inorg. Chem.* **2005**, 44, 4445.
- (30) Pyykkö, P.; Atsumi, M. *Chem. - Eur. J.* **2009**, 15, 186.
- (31) (a) Drover, M. W.; Bowes, E. G.; Schafer, L. L.; Love, J. A.; Weller, A. S. *Chem. - Eur. J.* **2016**, 22, 6793. (b) Brugos, J.; Cabeza, J. A.; García-Álvarez, P.; Kennedy, A. R.; Pérez-Carreño, E.; Van der Maelen, J. F. *Inorg. Chem.* **2016**, 55, 8905. (c) Stevens, C. J.; Dallanegra, R.; Chaplin, A. B.; Weller, A. S.; Macgregor, S. A.; Ward, B.; McKay, D.; Alcaraz, G.; Sabo-Etienne, S. *Chem. - Eur. J.* **2011**, 17, 3011. (d) Tang, C. Y.; Thompson, A. L.; Aldridge, S. *J. Am. Chem. Soc.* **2010**, 132, 10578.
- (32) (a) El-Hellani, A.; Kefalidis, C. E.; Tham, F. S.; Maron, L.; Lavallo, V. *Organometallics* **2013**, 32, 6887. (b) Rifat, A.; Patmore, N. J.; Mahon, M. F.; Weller, A. S. *Organometallics* **2002**, 21, 2856. (c) Crowther, D. J.; Borkowsky, S. L.; Swenson, D.; Meyer, T. Y.; Jordan, R. F. *Organometallics* **1993**, 12, 2897. (d) Núñez, R.; Viñas, C.; Teixidor, F.; Abad, M. M. *Appl. Organomet. Chem.* **2003**, 17, 509. (e) Riley, L. E.; Chan, A. P. Y.; Taylor, J.; Man, W. Y.; Ellis, D.; Rosair, G. M.; Welch, A. J.; Sivaev, I. B. *Dalton Trans.* **2016**, 45, 1127. (f) Mhinzi, G. S.; Litster, S. A.; Redhouse, A. D.; Spencer, J. L. *J. Chem. Soc., Dalton Trans.* **1991**, 2769.
- (33) (a) Shelly, K.; Finster, D. C.; Lee, Y. J.; Scheidt, W. R.; Reed, C. A. *J. Am. Chem. Soc.* **1985**, 107, 5955. (b) Shelly, K.; Reed, C. A. *J. Am. Chem. Soc.* **1986**, 108, 3117.
- (34) Teixidor, F.; Flores, M. A.; Viñas, C.; Sillanpää, R.; Kivekäs, R. *J. Am. Chem. Soc.* **2000**, 122, 1963.
- (35) Doi, J. A.; Teller, R. G.; Hawthorne, M. F. *J. Chem. Soc., Chem. Commun.* **1980**, 80.
- (36) (a) Bader, R. F. W. *Chem. Rev.* **1991**, 91, 893. (b) For QTAIM analysis of boron-containing clusters, carboranes, and electron-deficient cluster species, see: Bader, R. F. W.; Legare, D. A. *Can. J. Chem.* **1992**, 70, 657. (c) Bader, R. F. W. *Atoms in Molecules: A Quantum Theory*; Oxford University Press: New York, 1990.
- (37) (a) Swensen, J. S.; Polikarpov, E.; Von Ruden, A.; Wang, L.; Sapochak, L. S.; Padmaperuma, A. B. *Adv. Funct. Mater.* **2011**, 21, 3250. (b) Tsang, D. P.-K.; Chan, M.-Y.; Tam, A. Y.-Y.; Yam, W.-W. *Org. Electron.* **2011**, 12, 1114. (c) Veinot, J. G. C.; Marks, T. J. *Acc. Chem. Res.* **2005**, 38, 632.
- (38) Recently published methodology: (a) Dziedzic, R. M.; Saleh, L. M. A.; Axtell, J. C.; Martin, J. L.; Stevens, S. L.; Royappa, A. T.; Rheingold, A. L.; Spokoiny, A. M. *J. Am. Chem. Soc.* **2016**, 138, 9081. (b) Zhao, D.; Xie, Z. *Angew. Chem., Int. Ed.* **2016**, 55, 3166. (c) Lyu, H.; Quan, Y.; Xie, Z. *Angew. Chem., Int. Ed.* **2016**, 55, 11840. (d) Zhao, D.; Xie, Z. *Chem. Sci.* **2016**, 7, 5635. (e) Kabytaev, K. Z.; Everett, T. A.; Safronov, A. V.; Sevryugina, Y. V.; Jalisatgi, S. S.; Hawthorne, M. F. *Eur. J. Inorg. Chem.* **2013**, 2013, 2488. (f) Sevryugina, Y.; Julius, R. L.; Hawthorne, M. F. *Inorg. Chem.* **2010**, 49, 10627. (g) Lugo, C. A.; Moore, C. E.; Rheingold, A. L.; Lavallo, V. *Inorg. Chem.* **2015**, 54, 2094. (h) Kracke, G. R.; VanGordon, Y. V.; Sevryugina, Y. V.; Kueffer, P. J.; Kabytaev, K.; Jalisatgi, S. S.; Hawthorne, M. F. *ChemMedChem* **2015**, 10, 62. (i) Wingen, L. M.; Scholz, M. S. *Inorg. Chem.* **2016**, 55, 8274. (j) Cao, K.; Xu, T.-T.; Wu, J.; Jiang, L.; Yang, J. *Chem. Commun.* **2016**, 52, 11446. (k) Olid, D.; Núñez, R.; Viñas, C.; Teixidor, F. *Chem. Soc. Rev.* **2013**, 42, 3318. (l) Safronov, A.; Kabytaev, K. Z.; Jalisatgi, S. S.; Hawthorne, M. F. *Dalton Trans.* **2014**, 43, 12467. (m) Kabytaev, K. Z.; Safronov, A. V.; Jalisatgi, S. S.; Hawthorne, M. F. *J. Organomet. Chem.* **2014**, 749, 106. (n) Kabytaev, K. Z.; Safronov, A. V.; Sevryugina, Y. V.; Barnes, C. L.; Jalisatgi, S. S.; Hawthorne, M. F. *Inorg. Chem.* **2015**, 54, 4143. (o) Safronov, A. V.; Sevryugina, Y. V.; Jalisatgi, S. S.; Kennedy, R. D.; Barnes, C. L.; Hawthorne, M. F. *Inorg. Chem.* **2012**, 51, 2629. (p) Beletskaya, I. P.; Bregadze, V. I.; Kabytaev, K. Z.; Zhigareva, G. G.; Petrovskii, P. V.; Glukhov, I. V.; Starikova, Z. A. *Organometallics* **2007**, 26, 2340.
- (39) (a) Lavallo, V.; Wright, J. H., II; Tham, F. S.; Quinlivan, S. *Angew. Chem., Int. Ed.* **2013**, 52, 3172. (b) Kultyshev, R. G.; Liu, J.; Liu, S.; Tjarks, W.; Soloway, A. H.; Shore, S. G. *J. Am. Chem. Soc.* **2002**, 124, 2614. (c) Beletskaya, I. P.; Bregadze, V. I.; Ivushkin, V. A.; Petrovskii, P. V.; Sivaev, I. B.; Sjöberg, S.; Zhigareva, G. G. *J. Organomet. Chem.* **2004**, 689, 2920. (d) Kultyshev, R. G.; Lui, S.; Leung, H. T.; Liu, J.; Shore, S. G. *Inorg. Chem.* **2003**, 42, 3199. (e) Himmelsbach, A.; Reiss, G. J.; Finze, M. *Inorg. Chem.* **2012**, 51, 2679. (f) Douvris, C.; Michl, J. *Chem. Rev.* **2013**, 113, PR179. (g) Preetz, W.; Peters, G. *Eur. J. Inorg. Chem.* **1999**, 1999, 1831. (h) Semioshkin, A.; Brellochs, B.; Bregadze, V. *Polyhedron* **2004**, 23, 2135. (i) Olid, D.; Núñez, R.; Viñas, C.; Teixidor, F. *Chem. Soc. Rev.* **2013**, 42, 3318. (j) Peymann, T.; Knobler, C. B.; Hawthorne, M. F. *Inorg. Chem.* **2000**, 39, 1163. (k) Grüner, B.; Janoušek, Z.; King, B. T.; Woodford, J. N.; Wang, C. H.; Vřetečka, V.; Michl, J. *J. Am. Chem. Soc.* **1999**, 121, 3122. (l) Zhang, Y.; Liu, J.; Duttwyler, S. *Eur. J. Inorg. Chem.* **2015**, 2015, 5158. (m) Konieczka, S. Z.; Himmelsbach, A.; Hailmann, M.; Finze, M. *Eur. J. Inorg. Chem.* **2013**, 2013, 134. (n) Bolli, C.; Derendorf, J.; Jenne, C.; Scherer, H.; Sindlinger, C. P.; Wegener, B. *Chem. - Eur. J.* **2014**, 20, 13783. (o) Wong, Y. O.; Smith, M. D.; Peryshkov, D. V. *Chem. - Eur. J.* **2016**, 22, 6764. (p) Ivanov, S. V.; Lupinetti, A. J.; Solntsev, K. A.; Strauss, S. H. *J. Fluorine Chem.* **1998**, 89, 65. (q) Ivanov, S. V.; Davis, J. A.; Miller, S. M.; Anderson, O. P.; Strauss, S. H. *Inorg. Chem.* **2003**, 42, 4489. (r) *Boron Hydride Chemistry*; Muettterties, E. L., Ed.; Academic Press, Inc: New York, NY, 1975. (s) Ramírez-Contreras, R.; Bhuvanesh, N.; Zhou, J.; Ozerov, O. V. *Angew. Chem., Int. Ed.* **2013**, 52, 10313. (t) Press, L. P.; McCulloch, B. J.; Gu, W.; Chen, C.-H.; Foxman, B. M.; Ozerov, O. V. *Chem. Commun.* **2015**, 51, 14034. (u) Ramírez-Contreras, R.; Ozerov, O. V. *Dalton Trans.* **2012**, 41, 7842.